ISSN 1070-3632, Russian Journal of General Chemistry, 2010, Vol. 80, No. 3, pp. 576–590. © Pleiades Publishing, Ltd., 2010.
Original Russian Text © I.P. Suzdalev, 2010, published in Rossiiskii Khimicheskii Zhurnal, 2010, Vol. 53, No. 2, pp. 23–35.

Magnetic Phase Transitions in Nanoclusters and Nanostructures

I. P. Suzdalev

Semenov Institute of Chemical Physics, ul. Kosygina 4, Moscow, 119991 Russia
e-mail: suzdalev@chph.ras.ru

Received January 10, 2009

Abstract—Theoretical models and experimental data on magnetic phase transitions in magnetic nanoclusters and nanostructures were reviewed. It was shown that nanoclusters measuring from several nanometers to several tens of nanometers possess a critical size (which can be likened to the critical Curie or Neel temperatures). At undercritical cluster sizes the magnetic order in cluster and cluster nanostructure vanishes by first-order magnetic phase transitions (abruptly). In this context, a change-over from the first- to second-order magnetic phase transition, a decrease or increase in the Neel and Curie temperatures, and critical nanocluster size calculations were accomplished for a number of nanoobjects. These include ferric oxides and hydroxides in matrix nanostructures comprised of isolated nanoclusters, as well as in nanostructures including strongly interacting or organized clusters and in nanostructures induced by shear stress under high pressure loading.

DOI: 10.1134/S1070363210030394

INTRODUCTION

Basic research activities dedicated to magnetic phase transitions are of much importance for a number of technical applications. These transitions are typically classed with first- or second-order phase transitions, depending on how (abruptly or smoothly) the magnetization or magnetic ordering change near the critical point (Curie point for ferromagnetics and Neel point for anti- and ferrimagnetics). As for change in the unit cell volume of the magnetics and the heat effect of the first-order phase transition, they may be of both major and minor importance.

Most of bulk magnetics exhibit second-order phase transitions. However, some of them can develop first-order phase transitions, which is the case of a magnetically ordered–paramagnetic transition or a change in magnetic ordering. Examples can be found in MnAs (ferro → paramagnetic transition); MnO, UO_2, and Eu (antiferro → paramagnetic transition); and α-Fe_2O_3 (antiferro → weak ferromagnetic) [1, 2].

In nanoclusters and nanostructures, magnetic phase transitions are of special significance: Their nature and mechanism are influenced by many factors different from those in bulk materials, e.g., size-dependent effects, surface tension, intercluster and nanocluster–matrix interactions, magnetic fields, etc. Thus, studies of magnetic phase transitions offer a new tool for examination of the structural features of nanosystems and underlie development of new nanomaterials and nanodevices.

Nanoclusters and nanomaterials also exhibit first- and second-order magnetic phase transitions. Like in most bulk magnetics, second-order magnetic phase transitions in metal and metal oxide clusters are manifested as gradual disappearance of magnetic ordering and spontaneous magnetization near Curie T_C or Neel T_N points. Nanoclusters under 10 nm in size exhibit superparamagnetic properties, which leads to effective decreases in T_C or T_N. First-order magnetic transitions in nanoclusters of selected metal oxides are manifested as an abrupt disappearance of spontaneous magnetization at a certain temperature or at under-critical cluster size, which leads to transition of nano-clusters to paramagnetic, rather than superpara-magnetic, state [3–5].

Examination of first-order magnetic phase transitions in nanoclusters is complicated, above all, by the need in their differentiation from possible super-paramagnetism manifestations. Also, in most cases clusters vary in size or nanosystems do not form cluster crystals, which renders inevitable variation of

intercluster interactions. This complicates identification of first-order magnetic phase transitions in nanoclusters and nanostructures when examined via magnetization measurements providing averaged magnetic characteristics. In this context, a very promising tool for studying first-order magnetic phase transitions can be found in spectroscopic methods. They allow separately characterizing the magnetic and nonmagnetic fractions in one sample. In particular, this concerns Mössbauer spectroscopy with characteristic measurement times of 10^{-7}–10^{-10} s.

Magnetic phase transitions are differently manifested in isolated clusters (weak intercluster interactions) and nanosystems comprised of up to 100-nm clusters (strong intercluster interactions). In these two cases, the transitions are induced by different factors and follow different mechanisms. Hence, it is reasonable that magnetic phase transitions for nanosystems comprised of isolated small nanoclusters <10 nm in size be analyzed separately from those composed of larger strongly interacting clusters up to 100 nm in size.

Presented below is a discussion of the experimental and theoretically modeled data on magnetic phase transitions. Three nanosystem types were analyzed: (1) nanosystems comprised of isolated clusters; (2) nanostructures characterized by strong intercluster interactions, formed in the initial stage of nanocluster sintering, and nanostructures with cluster organization; and (3) nanostructures subjected to shear stress under high pressure loading. Comparison of theoretical results with experimental (primarily, ^{57}Fe and ^{151}Eu Mössbauer spectroscopic) data allowed the first-order magnetic phase transitions in nanostructures to be differentiated from possible manifestations of superparamagnetism and be properly characterized. Also, magnetic phase transitions were analyzed as influenced by intercluster and cluster–matrix interactions.

Nanosystems Comprised of Isolated Clusters

Magnetic ordering of a cluster is a collective phenomenon. For example, when embedded in a low concentration into a nonmagnetic, e.g., polymer matrix, single Fe atoms possessing a magnetic moment exhibit paramagnetic properties at all temperatures. Such clusters, even at a low Fe content of, e.g., less than ten Fe atoms, are characterized by exchange coupling, which, however, does not lead to spontaneous magnetization because of thermal fluctuations and fast spin–spin relaxations. A magnetically ordered cluster has the total magnetic moment and, consequently, the cluster size such that the total exchange energy exceeds the thermal fluctuation energy ($\sim kT$). Quantum statistics methods allow, in principle, calculating the total exchange energy for a cluster at a fixed position of its energy levels and, based on comparison with the thermal fluctuation energy, determining the critical cluster size (i.e., that beyond which the cluster loses spontaneous magnetization and magnetic ordering). However, precise calculation of the critical size of a cluster is a very difficult task. The reason is that the exchange coupling**,** and hence, the critical size of a cluster are affected by numerous factors, in particular, by the chemical condition of its surface, intercluster coupling, cluster shape, etc. The task can be simplified by restricting critical size estimation for a magnetic cluster to quantum limit calculation. Indeed, taking $\Delta p \Delta x = \Delta p d_{cr} \approx \hbar$ [where d_{cr} is the critical size (diameter) of the cluster; Δp, pulse uncertainty; Δx, coordinate uncertainty; and $\hbar$, reduced Planck constant], we obtain $\Delta p = \hbar/d_{cr}$. Hence, the uncertainty in determination of the electron, exchange coupling, or magnon energy, associated with quantum limit, can be expressed as

$$\Delta\varepsilon \approx (\Delta p)^2/2m \approx \hbar^2/2m\,(d_{cr})^2.$$

where m is the cluster mass.

By equating this energy to the exchange coupling energy which is primarily responsible for magnetic ordering, i.e., taking $\Delta\varepsilon \approx kT_C$ (T_C is the Curie point of the bulk material) we can obtain a simple expression for estimating the critical size:

$$d_{cr}(\text{in meters}) \approx 2\times10^{-8}\, T_C^{-1/2}, \quad (1)$$

For example, at T_C within 500–1000 K a magnetic cluster has the critical size $d_{cr} \approx 1$ nm. The same approach is applicable to assessing the lower limit of the cluster size in superparamagnetic state (the upper limit, close to 10 nm, is determined by numerous parameters, in particular, by magnetic anisotropy energy, temperature, measurement time, etc.). Thus, all clusters with $d < d_{cr}$ should occur in magnetically ordered state.

The critical cluster size can also be estimated in terms of the thermodynamic theory of magnetic phase transitions in nanoclusters [4]. This theory predicts first-order magnetic phase transitions and changes in transition order, depending on the nanocluster size.

In the case of bulk solids, first-order magnetic phase transitions can occur in materials for which the unit cell volume changes upon magnetic-nonmagnetic transitions. This concerns materials that exhibit

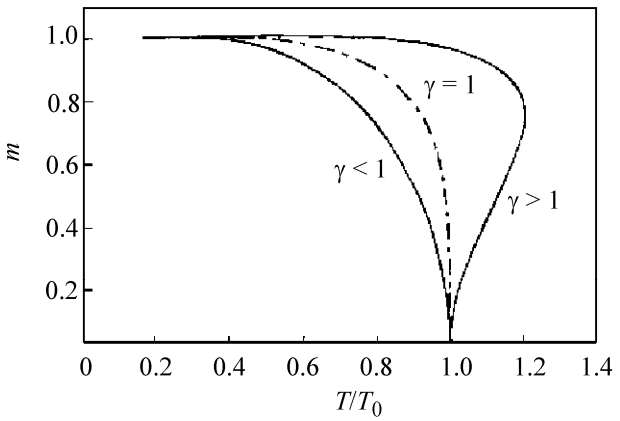

Fig. 1. Temperature dependence of relative magnetization of cluster at different γ values [see text, Eq. (5)].

magnetostriction (contraction under magnetic field exposure) and can experience hysteresis phenomena with respect to specific volume and magnetization under temperature changes [1, 2].

The model [4] describes the volume dependence of Curie (Neel) temperature as

$$T_C = T_0 [1 + \beta(V - V_0)/V_0], \quad (2)$$

where T_0 is the Curie temperature for a substance with uncompressed crystal lattice; $\beta = \partial(T_C - T_0)¤\partial(V - V_0)$, a constant associated with the change in magnetostriction; and V and V_0, molecular volumes in magnetically ordered (compressed) and nonmagnetic (paramagnetic) states, respectively.

A similar dependence is also taken for nanoclusters exhibiting first-order magnetic transitions.

Taking into account the cluster volume change associated with magnetostriction and surface tension-induced pressure $p = 2\alpha/R$ for a cluster with radius R, the Gibbs free energy per unit volume ΔG_V for magnetic-nonmagnetic transition is described by the equation

$$\Delta G_V = -1/2NkTm^2 + (1/2\eta)[(V - V_0)/V_0]^2 + 2\alpha/R(V - V_0)/V_0 + 1/2NkT [\ln (1 - m^2/4) + m\ln [(1 + m)/(1 - m)], \quad (3)$$

where N is the number of atoms with spin 1/2; $m = M/M_S$, relative magnetization; M_S, saturation magnetization; η, volume compressibility; and α, surface tension.

In this equation, the first, second, and third terms represent the exchange energy density, cluster deformation energy, and surface energy, respectively, and the fourth (entropy) term is responsible for Langevin-type temperature dependence of magnetization.

To derive an equation describing the stable magnetic state of a cluster, it is necessary to find the minimum of the free energy in relation to the volume and magnetization changes in magnetic phase transition. By solving a system of equations describing the equilibrium state of the system

$$\partial\Delta G_V/\partial V = 0 \text{ and } \partial\Delta G_V/\partial m = 0 \quad (4)$$

we can express the temperature dependence of the relative magnetization of a nanosystem as

$$T/T_{C0} = m(1/3\gamma m^2 + 1) / 1/2 \ln[(1 + m)/(1 — m)], \quad (5)$$

where γ is a parameter determining the magnetic phase transition order, $\gamma = (3/2)NkT_0\eta\beta^2/(1 - \eta\beta p)$, and $T_{C0} = T_0(1 - \eta\beta p)$, Curie temperature of the cluster. The latter parameter is smaller than T_0 because of the pressure p induced by the surface tension α of the cluster.

Figure 1 presents the calculated temperature (T/T_{C0}) dependences of the relative magnetization at different γ values. At $\gamma < 1$ the clusters undergo second-order magnetic phase transition, and at $\gamma \geq 1$, first-order magnetic phase transition (the magnetic order in the cluster abruptly vanishes). The Z-shaped section of the curve is indicative of a free energy increase, i.e., of the appearance of unstable magnetic structures. The dotted line indicates discontinuous variation of magnetization, which really corresponds to a first-order magnetic phase transition.

Using γ values it is also possible to estimate the critical size corresponding to discontinuous transition of the cluster from magnetically ordered to paramagnetic state.

It is convenient to represent γ as

$$\gamma = T_{CC}/T_{C0}, \quad (6)$$

where $T_{CC} = 3/2NkT_0^2\eta\beta^2$.

Hence, at $\gamma \geq 1$ the clusters undergo first-order magnetic phase transition to the paramagnetic state under condition

$$R \leq R_{cr} = 2\alpha\beta\eta / (1 - T_{CC}/T_0). \quad (7)$$

In large clusters ($R > R_{cr}$), magnetization vanishes with increasing temperature by second-order magnetic phase transition.

First-order magnetic phase transitions can occur in a cluster substances possessing sufficient compressibility η (clusters with zero compressibility are

characterized by R_{cr} = 0 and undergo second-order magnetic phase transitions). However, the appearance (disappearance) of first-order magnetic phase transitions and the critical cluster size [see Eqs. (5)–(7)] is primarily governed by the surface tension of cluster α. The phase transition model from [4] considers surface tension of an isolated cluster at the cluster/vacuum interface. Any interaction of a cluster with its stabilizing matrix and with its neighbor clusters causes decreases in α and R_{cr} and disappearance of first-order magnetic phase transitions. Thus, study of the latter allows characterizing the intercluster and cluster–interface interactions.

The first-order magnetic phase transitions in nanoclusters were experimentally examined with the use of a specially synthesized nanosystem comprised of ferric oxide-based nanoclusters $2.5Fe_2O_3 \cdot 4.5H_2O$ (this composition corresponds to mineral ferrihydrite), embedded into Polysorb matrix pores whose diameter ranges from 13 to 75 nm [4, 6]. This matrix nanosystem allows obtaining metal oxide clusters isolated from one another or concentrating several clusters in one pore. Polysorb (styrene-divinylbenzene copolymer) has hydrophobic pore walls, which significantly weakens the ferrihydrite cluster–matrix interaction and increases the critical cluster size. With pore size increasing from 13 to 75 nm the clusters in Polysorb pores also increase in size. The strength of intercluster interactions and the number of clusters contained in a pore were controlled by varying the Fe concentration in the Polysorb pores.

Figure 2 shows the Mössbauer spectra of ferrihydrite clusters in Polysorb pores, measured at different temperatures.[1]

All recorded spectra exhibited a magnetic hyperfine structure (HFS) comprising narrow lines and a paramagnetic central doublet. With increasing temperature a part of the HFS pattern is transformed to a paramagnetic doublet, which grows in intensity. This does not concern the broadening and shift of spectral line associated with superparamagnetic effects, resulting in a significant weakening of the magnetic field at the nucleus. Thus, ferrihydrite clusters undergo first-order magnetic phase transitions at 4.2–6 K.

[1] The cluster samples enriched in ^{57}Fe were synthesized in Polysorb pores by impregnation with an alcohol solution of $^{57}FeCl_3 \cdot 6H_2O$ (1.2×10^{-2} and 1.2×10^{-3} M), followed by Polysorb pore exposure to air with an ammonia admixture.

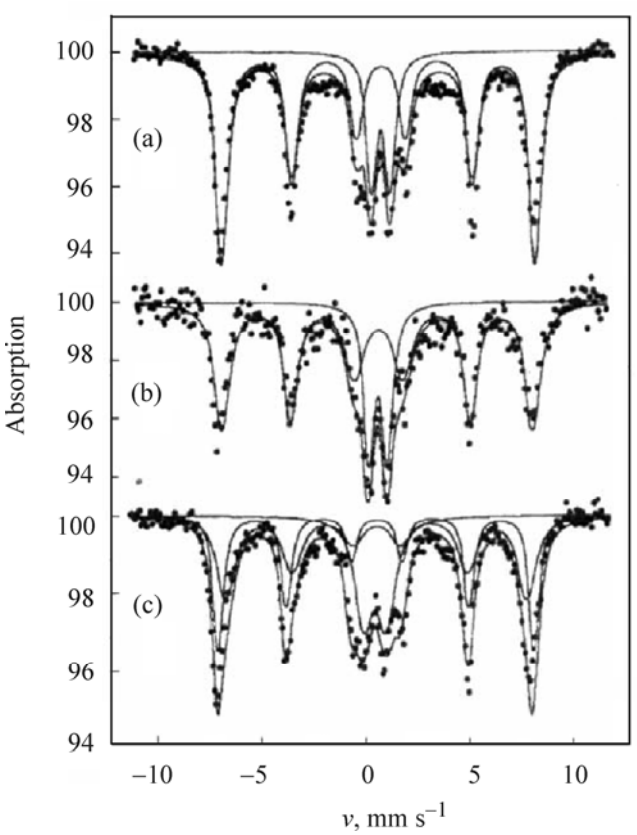

Fig. 2. Mössbauer spectra of ferrihydrite clusters in Polysorb with pore size of (a, b) 13 and (c) 20 nm. Cluster concentration $1.2\cdot10^{-3}$ M. Temperature of the sample, K: (a, c) 4.2 and (b) 10 K.

The Mössbauer spectra allow analyzing the magnetic phase transitions as influenced by the cluster–pore wall and intercluster interactions. Above all, ferrihydrite clusters in Polysorb are characterized by much narrower spectral lines (~0.6 mm s^{-1}) compared to 2–5-nm clusters of synthetic and natural ferrihydrites in magnetically ordered structures, exhibiting magnetic HFS patterns at 4.2 K and broad HFS lines (1.5–2 mm s^{-1}) in Mössbauer spectra [7]. This difference stems from the fact that ferrihydrite clusters are isolated from one another in the copolymer pores and is suggests that the cluster–pore wall and intercluster interactions are weaker than those in polycrystalline ferrihydrite. Indeed, the 1.2×10^{-3} M concentration corresponds approximately to one 1–2-nm ferrihydrite cluster in a pore with a volume of 10^{-22}–10^{-23} m^3. Therefore, the magnetic properties of the cluster will depend on the cluster–matrix surface interaction. Thus, even at 4.2 K the cluster undergoes a first-order magnetic phase transition, in which a part of the clusters having an undercritical size abruptly lose

spontaneous magnetization and pass to the paramagnetic state.

With pore size increasing to 20 nm (Fig. 2c), while the Fe atom concentration remains unchanged, the cluster increases in size. This increases the proportion of magnetic HFS and makes first-order magnetic phase transitions less probable. A tenfold increase in ^{57}Fe concentration, while the pore size remains unchanged, causes nucleation of several clusters in one pore (up to 5–8 clusters with a size of ~2 nm) [8] and enhancement of the intercluster interactions, which leads to an overall decrease in the critical size R_{cr} characteristic for first-order magnetic phase transitions. However, in the case of interest this effect allows estimating the size of the ferrihydrite clusters participating in superparamagnetic relaxation. Using the formula for magnetic relaxation

$$\tau_S = \tau_0 \exp(KV/kT), \quad (8)$$

where K is magnetic anisometry constant; V, cluster volume; and $\tau_0 = 10^{-9}$–10^{-10} s, the upper limit of cluster size was estimated at $R \approx 2.2$ nm for $c = 1.2\times10^{-2}$ M, $\tau_0 = 1\times10^{-9}$ s, $\tau_S \approx 189\times10^{-9}$ s, $T = 10$ K, and $K = 1.7\times10^5$ J m^{-3}.

Thus, the Mössbauer spectral data for the examined nanosystems are indicative of first- and second-order (superparamagnetism) magnetic phase transitions at 4.2–6 K for ~2-nm clusters. An increase to 75 nm in the pore size of the matrix with Fe-containing clusters embedded, while the cluster concentration remains unchanged (1.2×10^{-3} and 1.2×10^{-2} M), radically modfies the spectra [4]. Such nanosystem displays second-order magnetic phase transitions, with clusters exhibiting superparamagnetism solely. Superparamagnetic relaxation calculations allow estimating the cluster radius ($R \approx 2.2$ nm) for both concentrations, since the average pore size determines the average size of the cluster in the pore. An increase in Fe concentration leads to formation of several clusters in a pore, enhancement of intercluster interaction, and reduction in critical cluster size, which precludes first-order magnetic phase transitions.

It is of interest to compare the experimental R_{cr} values derived from the Mössbauer spectra and the estimated Fe atom concentrations in a pore with those calculated by formulas (5)–(7). The calculation utilized the following values of the characteristic parameters of the ferrihydrite clusters examined: the critical temperature of the first-order magnetic phase transition $T_{CC} = 4.2$–6 K, the temperature of the second-order magnetic phase transition (blocking temperature at which the area enclosed by the spectral component of the magnetic HFS pattern is equal to that of the doublet) for small clusters $T_0 \approx 20$–30 K; molecular volume of cluster $V_m = 14.4\times10^{-29}$ m^3; $1/\eta \sim 1.5\times10^{11}$ Pa; and $\alpha \approx 1$ J m^{-2}. This yielded $R_{cr} \approx 1$ nm, which agrees with the experimental value $R_{cr} \approx 1.5$–2 nm. Indications of first-order magnetic phase transitions were observed for small clusters of other Fe oxides (see, e.g., [5]). However, they were lacking for metal clusters (Fe, Co, Ni), possibly because of a lower compressibility of these materials.

An important factor responsible for the appearance (disappearance) of first-order magnetic phase transitions is pressure. The thermodynamic model of magnetic phase transitions nanoclusters [Eqs. (5)–(7)] predicts that the critical temperature will decrease with increasing external pressure as

$$T_{C0} = T_0(1 - \beta\eta p). \quad (9)$$

When the external pressure acting on the cluster p_0 changes by Δp, the magnetic transition temperature for a cluster changes by

$$\Delta T_{C0} = T_0[1 - \beta\eta(p_0 + \Delta p + 2\alpha/R)] - T_{C0}. \quad (10)$$

Hence,

$$\Delta T_{C0} = -T_0 \beta\eta\Delta p. \quad (11)$$

This suggests

$$\Delta T_{C0}/T_{C0} = \Delta p(2\alpha/R + p_0 - 1/\beta\eta)^{-1}. \quad (12)$$

At $p_0 << 2\alpha/R$ we can take

$$\Delta T_{C0}/T_{C0} = \Delta p\,(2\alpha/R - 1/\beta\eta)^{-1}. \quad (13)$$

Figure 3 presents the dependences of the relative magnetization on $T/T_{CC} = T/\gamma T_{C0}$ as calculated by formulas (5) and (12) for different pressures [9]. The p_6 pressure corresponds to $T/T_{CC} = 1$ ($\gamma = 1$) (first-order magnetic phase transitions), $p_7 = 0.95p_6$, to $T/T_{CC} = 1.2$ (second-order magnetic phase transitions), $p_5 = 1.05p_6$, to $T/T_{CC} = 0.8$, etc; $p_1 = 1.25p_6$ corresponds to $T/T_{CC} = 0$. The presented magnetization curves show that the phase transition temperature tends to decrease with increasing pressure. The calculations also suggest that an increase in pressure increases the probability for a cluster to pass to a nonmagnetic state via first-order magnetic phase transitions.

Thus, the pressure acting on the cluster nanosystem should cause decreases in the effective Curie and Neel temperatures for magnetic phase transitions.

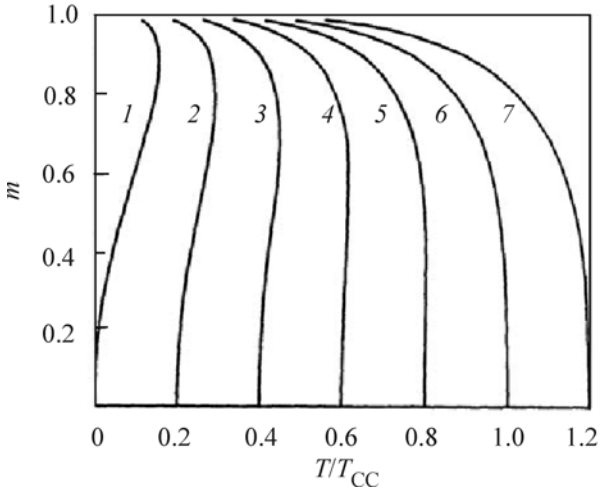

Fig. 3. Temperature dependences of relative magnetization of ferrihydrite clusters at different pressures: (*1*) $p_1 = 1.25p_6$, (*2*) $p_2 = 1.2p_6$, (*3*) $p_3 = 1.15p_6$, (*4*) $p_4 = 1.1p_6$, (*5*) $p_5 = 1.05p_6$, (*6*) $p_6 = 10^9$ Pa, and (*7*) $p_7 = 0.95p_6$.

The nanostructure hydration and freezing effects and the action on an isolated cluster of pressure generated by water freezing in nanopores were examined in a series of experiments. Their subjects were clusters of anhydrous and hydrated ferric oxyhydroxide FeO(OH) embedded into an ion-exchange resin (sulfocation exchanger).[2]

Like in the case of ferrihydrite, the Mössbauer spectroscopy offers an efficient tool for examining the magnetic phase transitions in ferric oxyhydroxide nanoclusters.

Figure 4 shows the Mössbauer spectra of nanoclusters of anhydrous and hydrated ferric oxy-hydroxide. The spectrum processing procedure in-volved isolation of a quadruple doublet and a hyperfine pattern, taking into account the magnetic field distribution.

The main distinction between the spectra of hydrated and anhydrous ferric oxyhydroxide nanoclusters is manifested at temperatures within 8.5–15 K. For example, in the case of freezing of the nanosystem, the contribution from the quadruple doublet increases at 10 K from 7.2 to 17.2%. Upon hydration, the central quadruple doublet grows in intensity. The spectra of anhydrous sulfocation exchanger samples containing

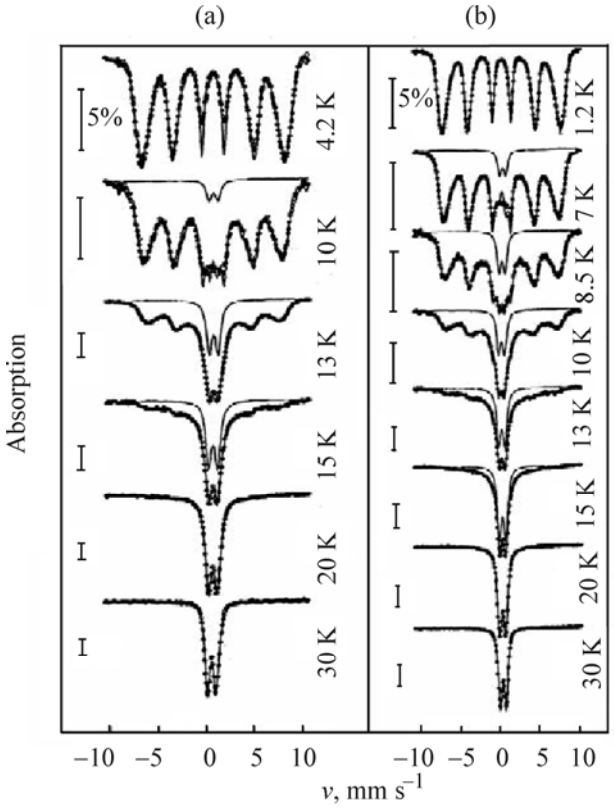

Fig. 4. Mössbauer spectra of ferric oxyhydroxide clusters in sulfocation exchanger: (a) anhydrous (water freezing in the cation exchanger pores) and (b) hydrated sample.

ferric oxyhydroxide clusters ($T = 13$ K, Fig. 4a) proved to be identical to those of hydrated samples ($T = 10$ K, Fig. 4b). Hence, hydration causes a temperature shift in the magnetic phase transition of the nanoobject, $\Delta T = 3$–4 K. This is a fully reversible phenomenon.

Let us briefly discuss in general the underlying mechanisms of hydration and freezing action on nanosystems and manifestations of the corresponding effects in Mössbauer spectra. Hydration of strongly swelling cation exchanger causes an increase in its volume, thereby increasing the distance separating the clusters embedded into the ion exchanger. This causes a decrease in the magnetic dipole energy of the intercluster interaction. Calculations show that, for 5-nm clusters, the magnetic dipole energy at the intercluster distance of 10 nm decreases relative to the contact arrangement to ca. 10^{-24} J. This value is by three orders of magnitude lower than the magnetic anisotropy energy of ca. 10^{-21} J). Thus, hydration does not affect the superparamagnetic relaxation period and cannot be responsible for the observed change in the Mössbauer spectrum.

[2] The ferric oxyhydroxide clusters (~3-nm) were prepared in KU-2 sulfocation exchanger pores by ion exchange from an aqueous solution of ^{57}Fe-enriched ferric chloride, followed by precipitation of the clusters with a NaOH solution [9].

The water freezing in the cation exchanger pores generates excess pressure acting on the cluster. This pressure is primarily determined by the polymer matrix deformation induced by waster crystallization. The stress developed in the matrix under strain is passed onto the cluster either directly or via the ice phase.

Calculation yielded $\Delta p = (0.45–9)\times10^9$ Pa for the excess pressure acting on the cluster in hydrated frozen organic matrix characterized by $1/\eta_m = (5–10)\times10^9$ Pa (where η_m is the matrix compressibility at the water crystallization temperature). This value is comparable with the surface tension-induced pressure acting on a cluster with the radius of 1.5 nm (at the surface tension $\alpha = 1$ J m^{-2} the pressure was estimated at $p\alpha = 2\alpha/R = 10^9$ Pa). This pressure can cause the magnetic anisotropy energy in the cluster to increase, especially in the case when a part of the cluster interacts with a polymer network segment. As might be expected, the superparamagnetic relaxation period will increase, thereby increasing the magnetic contribution to the hyperfine pattern and decreasing the contribution from the central doublet to the Mössbauer pattern. However, the experimental data contradict this presumption.

Analysis of this pressure-induced effect in terms of the thermodynamic model of magnetic phase transitions, with due regard to the pressure acting on the cluster [see Eqs. (5)–(7)], allows estimating the pressure-induced change in the temperature shift. The pressure growth causes the magnetic phase transition temperature to decrease by

$$\Delta T_{C0}/T_{C0} \sim (1/\eta_m)(2\alpha/R - 1/\beta\eta)^{-1}\Delta V/V, \qquad (14)$$

where ΔV is the cluster volume change, and V, cluster volume.

Let us take the following parameter values: $p\alpha \approx 10^9$ Pa, $\beta \approx 10^2$, $\eta \approx 10^{-11}$ m^2 J^{-1}, and $1/N \approx 10^{-28}$ m^3 (N is the number of atoms in the clusters examined). Hence, ΔT_{C0} can be expressed as

$$\Delta T_{C0} = (0.1 - 1.0)T_{C0}. \qquad (15)$$

Thus, a pressure-induced decrease in Curie temperature of the cluster, ΔT_{C0}, may be in the same order of magnitude with the T_{C0} value.

The ΔT_{C0} value estimated from the Mössbauer spectra (3–4 K, Fig. 4) is consistent with that derived from the thermodynamic calculation.

It should be noted that, in formula (14), the $\Delta T_{C0}/T_{C0}$ parameter is proportional to $\Delta V/V$, but the proportionality coefficient strongly depends on the $(2\alpha/R - 1/\beta\eta)^{-1}$ difference. Therefore, for a cluster with a specific size, at which it exhibits strong compressibility and magnetostriction properties, one can expect a significant increase in this coefficient, and, thereby, in the sensitivity to excess pressure. At fairly low pressures of 10^5–10^6 Pa this can induce a magnetic–nonmagnetic (paramagnetic) transition for a cluster. By contrast to the above-considered effects (they can all be interpreted in terms of the first-order magnetic phase transitions), the initial line broadening in the spectra of both anhydrous and hydrated samples can be due to superparamagnetic behavior of the clusters. As a result, such nanosystems can display magnetic phase transitions against the background of superparamagnetism.

Nanosystems Characterized by Intercluster Interactions

Nanosystems characterized by strong intercluster interactions undergo not only first- and second-order magnetic phase transitions (leading to disappearance of magnetic ordering and magnetization) but also magnetic transitions associated with changes in the magnetic structure and directions of magnetic moments.

Strong intercluster interactions can be stimulated by intercluster stresses and defects arising in nanosystems comprised of large (20–50-nm) nanoclusters. Such nanostructures are yielded by solid-phase chemical reactions, e.g., by cluster sintering, and also can be organized from monosized nanoclusters synthesized by micelle-template synthesis technique.

First-Order Magnetic Phase Transitions

First-order magnetic phase transitions similar to those in isolated ferrihydrite clusters (1–3-nm) were observed in a nanosystem comprising α- and γ-Fe_2O_3 [10], formed in the initial stage of cluster sintering in a solid-phase reaction [11]. Figure 5 shows the atomic-force microscopic images of this nanostructure.

Figure 6 presents the Mössbauer spectra of the nanosystem comprised of α- and γ-Fe_2O_3, measured at different temperatures. They demonstrate the evolution of a magnetic phase transition from magnetically ordered (magnetic HFS) to a paramagnetic (superparamagnetic) state of the nanostructure. The spectrum recorded at 77 K consists of two magnetic hyperfine patterns corresponding to α- (quadruple shift $\Delta E_Q = -0.29$ mm s^{-1}) and γ-Fe_2O_3 ($\Delta E_Q = 0$ mm s^{-1}). With temperature increased to 120 K, a quadruple doublet ($\Delta E_Q = 0.78$ mm s^{-1}) appears in the spectrum. It

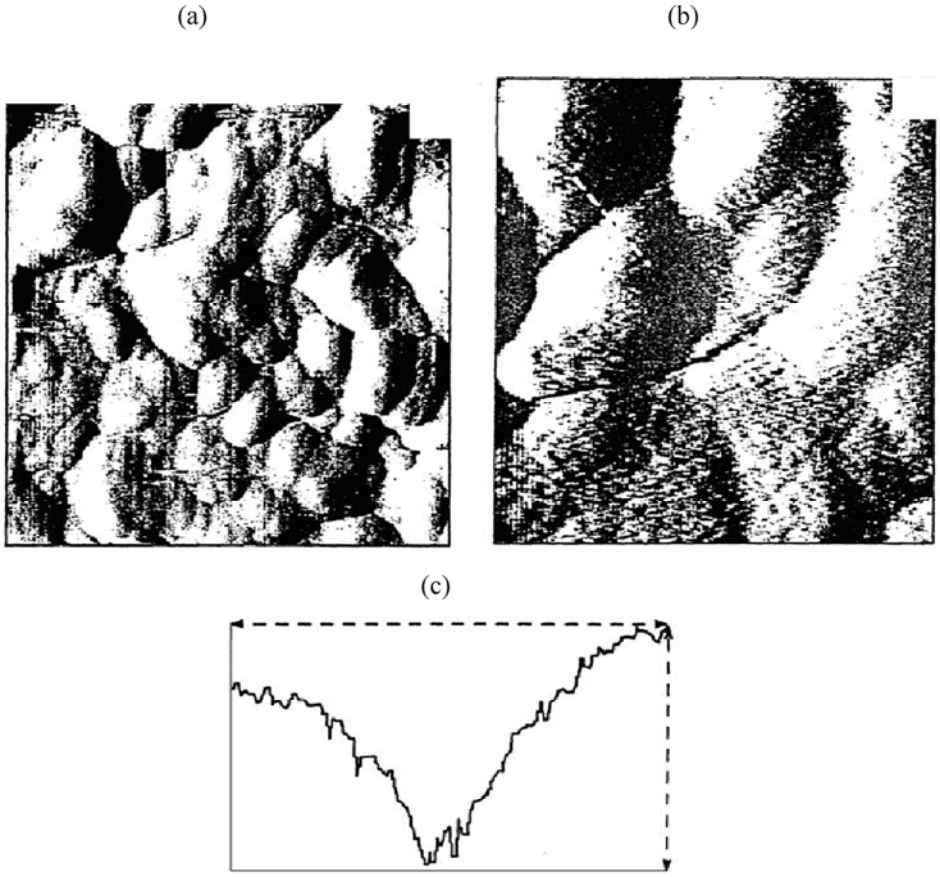

Fig. 5. (a, b) AFM profiles of α-, γ-Fe_2O_3 nanoclusters on (a) 500- and (b) 150-nm scale and (c) surface relief. The relief is shown for a sector along the dashed line drawn in the left segment of Fig. 5b; line length 14 nm; maximal depth of relief 6.4 nm.

exhibits an isomer shift relative to Fe metal (δ = 0.42 mm s^{-1}), but the general spectral pattern remains unchanged. Further increase in temperature causes transformation of the spectrum into a single magnetic hyperfine pattern (ΔE_Q = 0 mm s^{-1}). The Mössbauer spectra recorded at 120–300 K are indicative of reversible transformations of the magnetic HFS into a paramagnetic doublet without noticeable shift or broadening of lines characteristic for second-order magnetic phase transitions or for superparamagnetism. This suggests the occurrence of first-order magnetic phase transitions (discontinuous disappearance of magnetization).

First-order phase transitions in the nanostructures occur at critical temperatures T_{C0} within 120–300 K, which are lower than T_0 for bulk α- and γ-Fe_2O_3 samples (856 and 965 K, respectively). Calculations by formula (8) suggest the lack of superparamagnetism for such large clusters. Taking the magnetic anisotropy constant $K \approx 10^5$ J m^{-3} and $\tau_0 = 10^{-9}$–10^{-10} s, we will obtain the magnetic moment relaxation time τ that exceeds by several orders of magnitude the measurement time (Larmor precession time for ^{57}Fe is ~10^{-8} s).

Thus, superparamagnetism does not affect the magnetic properties of the considered nanostructures and thus cannot be responsible for a decrease in T_{C0}. The magnetization and magnetic order for α- and γ-Fe_2O_3 nanostructures vanish by first-order magnetic phase transition (abruptly), with the magnetic induction $B_{in} \approx 50$ T changing to 0 T. It should be noted that isolated ferrihydrite clusters are characterized by the critical size $R_{cr} \approx 1.5$ nm [4] (cluster size decreasing beyond the critical value causes discontinuous transition of the cluster to the paramagnetic state). Such clusters are also characterized by a narrow temperature range within 4.2–6 K typical for first-order phase transitions. These effects are caused by surface tension-induced pressure.

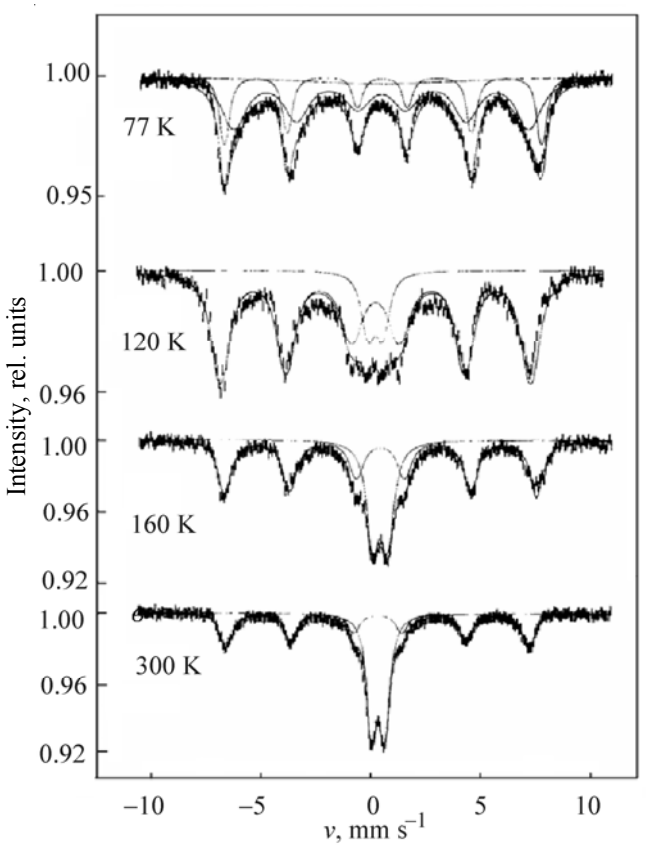

Fig. 6. Mössbauer spectra of α-, γ-Fe_2O_3 nanostructure at different temperatures.

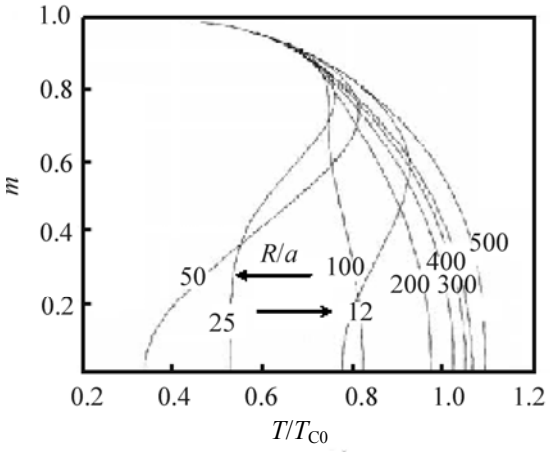

Fig. 7. Temperature dependence of relative magnetization of ferric oxide at different cluster radius/lattice constant ratios (R/a).

In the case of 20–50-nm clusters the surface tension-induced pressure should be by an order of magnitude lower. Moreover, the surface tension is decreased because of strong intercluster interactions. Hence, some different factors should be responsible for magnetic phase transitions and decreases in T_{C0}, corresponding to $\gamma \geq 1$ [γ determines the phase transition order, see formula (5)] in such nanostructures. These factors should be associated with the influence exerted by defects on the properties of nanostructure [12]. It is believed that, among ferric oxide clusters, the maximal defect density is characteristic for 20–50-nm clusters. For larger clusters, surface is a poor source of defects. At the same time, for smaller clusters the surface tension is sufficient for "squeezing out" defects from the cluster, which allows treating small clusters as having no defects [13].

In terms of this model, there should exist a maximal density of defects with its corresponding critical cluster size (ca. several tens of nanometers), determining the magnetic state of the nanostructure: At smaller sizes the cluster undergoes first-, and at larger, second-order magnetic phase transitions, with the latter being typical for bulk materials.

The maximum in the defect concentration–cluster size dependence [12, 13] has a characteristic manifestation in the temperature dependences of the magnetization for nanocluster systems comprising clusters of different sizes. The dependence of the critical temperature on the defect concentration in a cluster can be taken as linear

$$T_C = T_{C0}(1 + \beta c_V), \quad (16)$$

where $\beta < 0$, and c_V is the defect concentration in a cluster.

With magnetic interaction of the clusters taken into account, the thermodynamic potential of a magnetic clusters–medium–defects nanosystem can be represented by the sum of the surface energy of the cluster and the change in the chemical potential with changing cluster size and defect density in the cluster

$$G = \Delta\mu n_V + \alpha s(n_V) - 0{,}5N_V kT_{C0}(1 + \beta c_V)m^2$$
$$+ NkT\{0.5\ln[(1 - m^2)/4] + mln[(1 + m)/(1 - m)]\}, \quad (17)$$

where $\Delta\mu = \mu_0 + kT \ln (N_S n_V / N_V n_S)$ is the difference of the chemical potentials for defects in the bulk and on the surface of the cluster, respectively; N_V, number of atoms in the cluster; N_S, number of atoms in the intercluster medium per cluster; n_V, number of defects in the cluster; n_S, number of defects in the intercluster medium per cluster; α, surface tension of the cluster in the intercluster medium; s, surface area of the cluster; $m = M/M_S$, relative magnetization of the cluster; and N, number of spins in the cluster.

The energy-minimization conditions $\partial\Delta G_V/\partial c_V = 0$, $\partial\Delta G_V/\partial m = 0$ and equilibrium state identification yield the temperature dependence of the magnetization for clusters with different sizes [14] (see examples for ferric oxide in Fig. 7).

The temperature dependence of magnetization [formula (16)] is consistent with the data from [13, 14] and the predicted existence of a critical size for 30–40-nm oxide clusters, corresponding to the maximal defect density in the cluster. Above and below this critical value, clusters undergo second- rather than first-order magnetic phase transitions.

Nanostructures synthesized by microemulsion- and template-assisted techniques, as well as by reverse-micellar procedure as a mesophase (liquid crystals), followed by slow annealing, exhibit pronounced cluster organization [15]. Figure 8 presents the Mössbauer spectra of the nanocluster structure synthesized with the use of a template, a mesophase with 20% surfactant, followed by slow annealing at 350°C. Like in the case discussed above, the spectra consist of two magnetic hyperfine patterns corresponding to the twinning nanostructure of α- and γ-Fe_2O_3 (isomer shift $\delta = 0.45 \pm 0.03$ mm s^{-1}) and γ-Fe_2O_3 nanostructure ($\delta = 0.48 \pm 0.03$ mm s^{-1}). Also, the spectra measured at 166 and 300 K contain a quadruple doublet ($\delta = 0.36 \pm 0.03$ and $\delta = 0.32 \pm 0.03$ mm s^{-1}). The lacking or minor broadening of the magnetic HFS lines suggests weak magnetic relaxation and superparamagnetism. The Mössbauer patterns are indicative of first-order magnetic phase transitions at 166 and 300 K in such nanostructures. The manifestation of these transitions, along with discontinuous growth of magnetization till saturation at magnetic field inductions of several fractions of Tesla, also validates the nanocluster organization of the ferric oxide nanoparticles. For comparison, in disordered nanosystem comprised of Fe_2O_3 clusters in a NaCl matrix, the magnetization smoothly grows and does not attain saturation in fields with magnetizations of up to 1 T [15].

Nanoclusters with template-organized structure (10–20-nm) are not sufficiently small for the surface tension to provide the pressure needed for initiating first-order magnetic phase transitions and to lead to noticeable compression of the crystal lattice [4]. First-order magnetic phase transition [$\gamma \geq 1$, see formula (5)] in such nanocluster systems requires much higher compressibilities than those in covalent or ionic crystals.

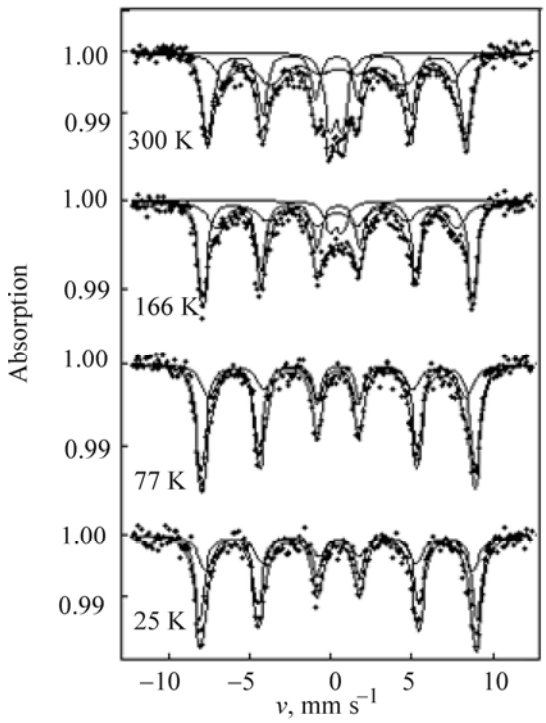

Fig. 8. Mössbauer spectra at different temperatures for ferric oxide nanostructure synthesized by micelle-template technique.

This compessibility corresponds to the cluster-organized nanostructure (cluster crystal), similar to inert gas crystal.

Weak Ferromagnetic → Antiferromagnetic Collective Magnetic Phase Transitions and Formation of Twin Nanostructures

Some antiferromagnetics, in particular, α-Fe_2O_3, $MnCO_3$, $CoCO_3$, and MnF_2 crystals, as well as orthorhombic crystals with rare-earth ferrite structure $MFeO_3$ (M is rare-earth element) exhibit weak ferromagnetism [1]. This is associated with a weak noncollinearity of spins in the antiferromagnetic sublattice. This noncollinearity was calculated with due regard to weak magnetic coupling; it arises with increasing temperature because of unstable compensation of the total magnetic moment of the antiferromagnetic [16].

Let us consider a nanosystem comprising α- and γ-Fe_2O_3 clusters, of which γ-Fe_2O_3 phase has a cubic spinel structure, and α-Fe_2O_3, a corundum structure with a rhombohedral lattice. Bulk α-Fe_2O_3 exhibits a magnetic phase transition known as Morin transition; it is characterized by $T_M \approx 260$ K corresponding to discontinuous change in magnetic ordering. For

example, $T < 260$ K corresponds to collinear antiferromagnetism, and $T > 260$ K, to noncollinear antiferromagnetism (weak ferromagnetism). This transition is associated with the specific internal symmetry of the crystal, whose lattice can undergo distortion with increasing temperature, which is accompanied by atomic spin rotation by 90°. The collinearity-noncollinearity transition for magnetic moments of sublattices is identified from changes in sign and magnitude of quadruple splitting of the Mössbauer HFS lines.

The high-temperature α-Fe_2O_3 phase is characterized by the quadruple shift $E_Q = +0.2$ mm s^{-1}, and a low-temperature phase, by $\Delta E_Q = -0.3$ mm s^{-1}. The specific feature of the weak ferromagnetic → antiferromagnetic transition in a nanosystem comprising α- and γ-Fe_2O_3 can be derived from the quadruple ΔE_Q and isomer δ shift data presented in Fig. 9.

The low-temperature α-Fe_2O_3 phase corresponds to collinear antiferromagnetic, which undergoes transition to noncollinear magnetic with $\Delta E_Q = 0.0$–0.1 mm s^{-1} above 120 K. Thus, the transition temperature for this nanosystem decreases to $T_M \approx 120$ K; the high-temperature phase is characterized by a lower ΔE_Q. Therefore, the α- and γ-Fe_2O_3 nanostructures undergo discontinuous, first-order, magnetic phase transition, collinear → noncollinear ferromagnetic (the latter exhibits weak ferromagnetism). A decrease in T_M is associated with the specific ratio of the magnetic dipole (E_M) and exchange (E_{Ex}) energies. Indeed, the collinearity angle can be represented as $\alpha \sim E_M/E_{Ex}$ [16], and a decrease in E_{Ex} with decreasing cluster size (as suggested by a decrease in T_{C0} for the nanosytem) increases the probability of noncollinear antiferromagnetism. As a result, a Morin transition occurs already at 120 K.

An essential feature of the Morin transition in nanostructures consists in the following: Despite broad size distribution of the clusters, the phase transition occurs at a fixed temperature ($T_M \approx 120$ K) without intermediate temperatures which can range in very large clusters from T_M of 260 K to 120 K. This suggests transformation of the entire nanostructure, with a phase transition in one cluster initiating that in the entire system. An example of such transitions involving collective transformations can be found, e.g., in austenite–martensite (martensitic) transitions in carbonaceous steels [17].

Let us turn back to Fig. 9. At low temperatures $T <$ 120 K the nanostructure contains both α-Fe_2O_3 and γ-Fe_2O_3 phases. Above 120 K, along with Morin (antiferromagnetic → weak ferromagnetic) transition,

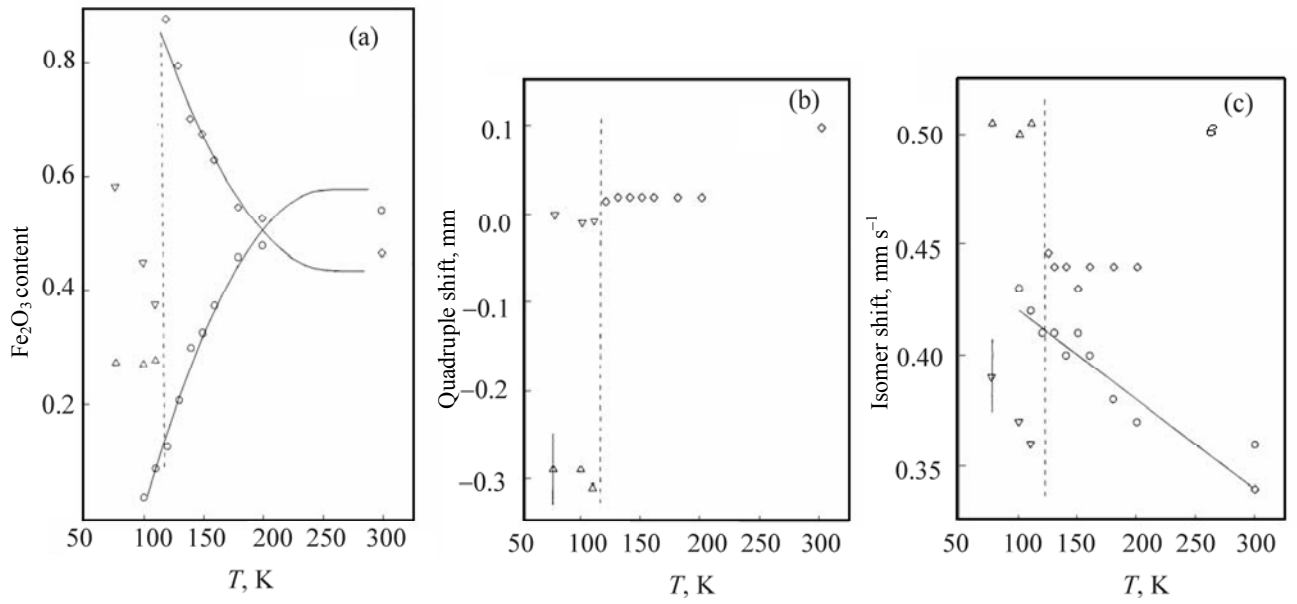

Fig. 9. Simulated Mössbauer spectra of α-, γ-Fe_2O_3 nanostructure: Temperature dependence of (a) spectral area, (b) quadruple shift ΔE_Q for magnetic HFS, and (c) isomer shift δ for different Fe_2O_3 phases in the nanosystem: (○) paramagnetic phase (quadruple doublet), (∇) γ-Fe_2O_3 magnetic phase, (Δ) α-Fe_2O_3 magnetic phase, and (◊) twin Fe_2O_3 magnetic phase. Dotted line designates the phase transition area.

bulk oxide samples undergo formation of one common phase from α-Fe_2O_3 and γ-Fe_2O_3 at 256 K. The parameter ΔE_Q for this phase is close to that in α-Fe_2O_3, with both α-Fe_2O_3 and γ-Fe_2O_3 phase structures preserved (according to X-ray diffraction data). The temperature dependences of the isomer shift δ (see Fig. 9c) are indicative of its abrupt change at 120 K: The isomer shift for the α phase decreases, and that for γ phase, increases discontinuously to the average value of δ = 0.45 mm s^{-1}. This suggests collective transformations of γ-Fe_2O_3 and α-Fe_2O_3 phases into an α-type phase preserving the cubic spinel symmetry of the nanostructure, which can be explained by formation of a twin structure. It should be noted that twinning phenomenon, known for crystallization, mechanical strains, and sintering of nuclei, is induced by fast thermal expansion or contraction, as well as by heating of strained crystals [18].

Nanostructures Subjected to Shear Stress Under High Pressure Loading

Shear stress exposures under high pressures lead to formation of nanostructures comprised of 5–10-nm nanocrystallites in bulk materials [19]. Simultaneous plastic strain generates numerous defects modifying the magnetic properties of the nanostructures, in particular, the order and critical parameters of magnetic phase transitions. For example, the resulting nanocomposites comprising α- and γ-Fe_2O_3 nanoclusters (which allow the nanosystem to retain the stress and defects after the pressure and shear strength are removed) can exhibit first-order magnetic phase transitions and further decrease in critical temperatures T_{C0} because of an increase in defect density [12–14]. Formation of nanostructures in bulk solids should also cause a change in the magnetic phase transitions order (from first to second and vice versa).

Let us discuss the data on magnetic phase transitions as influenced by shear stress under high pressure loading for two nanosystem types: those based on α- and γ-Fe_2O_3 nanoclusters (nanosystem 1) and on metallic europium (nanosystem 2). Nanosystem 1 includes 20–50-nm α- and γ-Fe_2O_3 nanoclusters (nanosystem 1.1) or 20–50-nm α- and γ-Fe_2O_3 nanoclusters with 50% acrylamide monomer addition (nanosystem 1.2). Nanosystem 2 is comprised of samples of metallic Eu (nanosystem 2.1), or metallic Eu with 1% addition of 20–50-nm α- and γ-Fe_2O_3 nanoclusters (nanosystem 2.2), or metallic Eu with 10% adamantane addition (nanosystem 2.3) [13, 14].

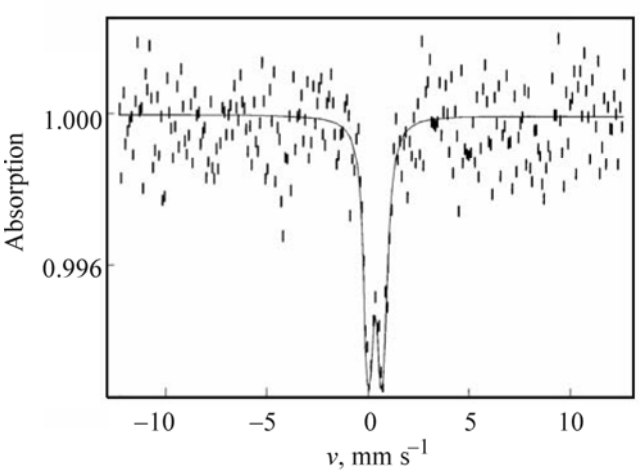

Fig. 10. Room-temperature ^{57}Fe Mössbauer spectrum of nanostructure 2.2 subjected to shear stress under pressure loading of 2 GPa. Anvil shift angle 240°.

A high-pressure installation with Bridgman anvils allowed generation of up to 5 GPa pressures and simultaneous accumulation of the net shift with 10° step-by-step change within 5 s.

Shear stress exposure under up to 2 GPa pressures induces polymerization of acrylamide in system 1.2. This allows the shear strains to be preserved after stress is removed from samples of α- and γ-Fe_2O_3 nanoclusters**,** thereby precluding their recrystallization and recovery of the initial phase equilibrium. Shear stress exposures under high pressure loading cause the contribution from the nonmagnetic component in system 1.2 to increase, with the most impressive result obtained for system 2.2.

The ^{57}Fe Mössbauer spectrum of nanostructure 2.2, recorded at 300 K upon shear stress exposure under high pressure loading (Fig. 10), is indicative of virtually complete loss of magnetic order by α- and γ-Fe_2O_3 clusters. This suggests decreases in the average cluster size, as well as in the Curie or Neel temperature (beyond room temperature).

The Mössbauer spectra for nanosystems based on metallic europium (Fig. 11) revealed the opposite trend: The magnetic phase transition temperature increases for europium. Along with four HFS lines associated with metallic Eu component, the spectrum of nanostructure 2.1 (Fig. 11a) contains lines of Eu_2O_3 and EuO. The spectrum of nanosystem 2.2 (Fig. 11b) contains three components: a broad line associated with metallic Eu and lines of EuO and Eu_2O_3. The

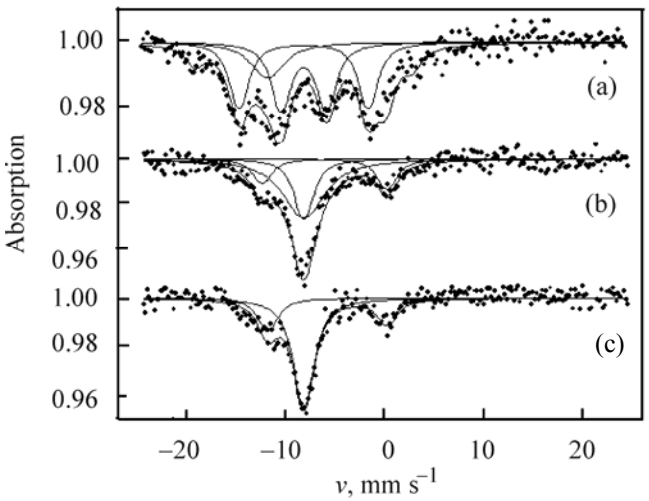

Fig. 11. ^{151}Eu Mössbauer spectra (T = 90 K) of nanostructure (a) 2.1, (b) 2.2, and (c) 2.3 subjected to shear stress under pressure loading of 2 GPa. Anvil shift angle 120°.

spectrum of nanostructure 2.3 comprises three components, specifically the hyperfine pattern of magnetically ordered metallic Eu, a very broad monoline corresponding to metallic Eu, and a monoline of EuO (Fig. 11c).

The discussed experimental results suggest the following:

(1) Nanostructures 1.1, 1.2, and 2.2 subjected to shear stress under high pressure exhibit first-order magnetic transitions: The magnetization vanishes abruptly at a certain critical temperature. This is associated with the fact that, with temperature increasing from 77 to 300 K, the α- and γ-Fe_2O_3 nanoclusters in these nanosystems undergo transitions from a magnetic state characterized by magnetic HFS to a paramagnetic state without line broadening and shifting, as associated with the existence of a critical cluster size.

(2) Nanostructures 1.1 and 1.2, as well as system 2.2 comprising α-Fe_2O_3 and γ-Fe_2O_3, are characterized by critical temperatures of the magnetic phase transitions (T_C or T_N), that are much lower than those for bulk samples. Introduction of acrylamide (nanostructure 1.2) and metallic Eu (nanostructure 2.2) causes even stronger decreases in critical temperatures of magnetic phase transitions in the clusters.

(3) Nanostructure 2.1 loaded with metallic Eu displays a second-order magnetic phase transition (by contrast to α-Fe_2O_3 and γ-Fe_2O_3 nanostructures). This follows from the fact that, above the critical (transition) temperature (~80 K [18]), a narrow line associated with nonmagnetic Eu is superposed in the spectrum with a broad contour corresponding to unresolved magnetic hyperfine pattern associated with magnetically ordered Eu. Thus, the magnetic phase transition temperature T_N for nanostructured Eu, ~100 K, is higher than that for bulk metallic Eu.

(4) Nanosystems 2.2 and 2.3 exhibit further increase in T_N (especially pronounced for nanosystem 2.3) upon adding 1% α- and γ-Fe_2O_3 nanoclusters (system 2.2) or 10% adamantane (system 2.3) to metallic Eu.

All these aspects of magnetic behavior are characteristic for nanostructures comprising fairly large nanoclusters, which preserve high density of defects generated by shear stress under high pressure loading. Therefore, studies of defect distribution in a nanostructure characterized by a maximal defect density for 30–50-nm clusters allow characterizing the magnetic properties of nanostructures. These critical defect densities should correspond to the critical cluster sizes observed in change-over from the first to second (and vice versa) order for magnetic phase transition.

The model of magnetic phase transitions in nanostructured systems including defects [13, 14] allows interpreting all the above-considered effects observed for both oxide and metal nanosystems.

For 20–50-nm ferric oxide clusters, first-order magnetic phase transitions should be observed. Magnetization of such clusters vanishes abruptly at temperatures above the Curie point T_C. Also, T_C varies with the size of the clusters constituting the system. At cluster size exceeding the maximal critical value ($> R_{cr}$) the system undergoes a second-order magnetic phase transition characteristic for bulk samples, and T_C increases. On the other hand, a decrease in size ($< R_{cr}$) also leads to second-order magnetic phase transitions because of a decrease in the defect concentration.

The magnetic phase transition order and T_C are affected by intercluster magnetic interaction. However, the intercluster distance has a less pronounced effect on the temperature dependence of magnetization than does the cluster size. For example, a decrease in the intercluster distance relative to the value corresponding to the lattice constant causes T_C to increase by ca. 6% at most [14]. This is paralleled by a change-over from the first- to second-order magnetic phase transitions.

Shear stress exposures under high pressure loading are responsible for another essential feature of magnetic behavior of the nanosystems. Specifically, pressure induces further nanostructurization: Decreases are observed both in average cluster size and average intercluster distance. In nanosystem 1.1 comprised of α-Fe_2O_3 and γ-Fe_2O_3, the effect exerted by the decrease in the cluster size on T_C is compensated by compaction which strengthens the magnetic interaction of the clusters. For nanosystem 1.2 containing a polymer addition, as well as for nanosystem 2.2, T_C tends to decrease, and the contribution from the first-order magnetic phase transition, to increase. This phenomenon is especially prominent for nanosystem 2.2 in which the magnetic order for all α-Fe_2O_3 and γ-Fe_2O_3 nanoclusters vanishes at room temperature. Thus, a decrease in intercluster distance causes enhancement of magnetic interactions and renders more probable first-order magnetic phase transitions.

In sample 2.1 (metallic europium) the shear stress exposure under high pressure loading induces the following effects. At temperatures below the Neel point T_N the initial Eu metal has a domain structure in which the domain size reaches tens of nanometers [1, 20]. At temperatures above $T_N \approx 80$ K the system undergoes a first-order magnetic phase transition, and magnetic order in bulk metallic Eu vanishes abruptly. In the magnetically ordered state the metallic europium structure is regarded as consisting of domain nanoclusters packed into the crystal lattice of metallic Eu. When the size of these magnetic domain nanoclusters is close to 20–30 nm, the peak density of defects and, hence, of stresses, is achieved. This is specifically responsible for first-order magnetic phase transitions in metallic Eu. These conclusions were validated by high magnetostriction coefficients of rare-earth metals.

Shear stress exposure under high pressure loading causes a decrease in size of domain clusters to an undercritical value, thereby decreasing the defect concentration and removing stresses in the metal. As a result, first-order magnetic phase transition does not occur, and the magnetically ordered state is "drawn" to higher temperatures. This is responsible for an increase in the Neel temperature in nanostructured metallic europium. Adding 1% ferric oxide clusters to metallic Eu causes enhancement of this effect. The reason lies in higher shear strains in ferric oxides compared to metallic Eu, which causes the nanoclusters in the nanosystem to decrease in size. Higher effects are achieved upon introduction into europium matrix of adamantane molecular clusters with which the stresses are preserved in the nanostructure upon pressure is removed. Moreover, introduction of ferric oxide and adamantane molecular clusters is apparently conducive to uniform nanostructurization under shear stress exposure with high pressure loading.

Thus, nanostructurization of substances can lead to both decreases and increases in the critical temperatures T_C (T_N) in nanomaterials.

CONCLUSIONS

The nanocluster critical size is the factor responsible for magnetic phase transitions in nanoclusters, by contrast to bulk materials. At undercritical cluster sizes, the nanosystems undergo discontinuous transition to a nonmagnetic state. Such phase transitions are characterized by a decrease in Curie or Neel temperature (in the case of first-order magnetic phase transitions) or an increase in critical temperatures (in the case of second-order magnetic phase transitions).

ACKNOWLEDGMENTS

This study was financially supported by the Russian Foundation for Basic Research (project nos. 06-03-32006 and 09-03-00023).

REFERENCES

1. Vonsovskii, S.V., *Magnetizm* (Magnetism), Moscow: Nauka, 1971.
2. Bean, C.B. and Rodbell, D.S., *Phys. Rev*., 1962, vol. 126, p. 104.
3. Suzdalev, I.P., *Fiz. Tverd. Tela*, 1970, vol. 12, p. 988.
4. Suzdalev, I.P., Buravtsev, V.N., Imshennik, V.K., Maksimov, Yu.V., Matveev, V.V., Novichikhin, S.V., Trautwein, A.X, and Winkler, H.Z., *Physica D*, 1996, vol. 37, p. 55.
5. Suzdalev, I.P. and Suzdalev, P.K., *Usp. Khim*., 2001, vol. 70, p. 203.
6. Suzdalev, I.P. and Trautwein, A.X., *Khim. Fiz*., 1996, vol. 15, p. 96.
7. Murad, E. and Johnston, J.H., *Modern Inorganic Chemistry. Moessbauer Spectroscopy Applied to Inorganic Chemistry*, Long, G.J., Ed., New York: Plenum, 1987, vol. 2.
8. Suzdalev, I.P., Buravtsev, V.N., Imshennik, V.K., and Novichikhin, S.V., *Khim. Fiz*., 1993, vol. 12, p. 555.
9. Suzdalev, I.P., Plachinda, A.S., Buravtsev, V.N., Maksimov, Yu.V., Reiman, S.I., Khromov, V.I., and Dmitriev, D.A., *Khim. Fiz*., 1998, vol. 17, p. 104.

10. Suzdalev, I.P., Maksimov, Yu.V., Novichikhin, S.V., Buravtsev, V.N., Imshennik, V.K., and Matveev, V.V., *Khim. Fiz*., 2000, vol. 19, p. 105.
11. Suzdalev, I.P., Maksimov, Yu.V., Novichikhin, S.V., Buravtsev, V.N., Kazakevich, A.G., Imshennik, V.K , and Matveev, V.V., *Kolloid. Zh*., 2000, vol. 62, p. 257.
12. Suzdalev, I.P., Buravtsev, V.N., Imshennik, V.K., and Maksimov, Yu.V., *Scr. Mater*., 2001, vol. 44, p. 1937.
13. Suzdalev, I.P., Buravtsev, V.N., Maksimov, Yu.V., Zharov, A.A., Imshennik, V.K., Novichikhin, S.V., and Matveev, V.V., *Izv. Ross. Akad. Nauk, Ser. Khim*., 2003, p. 1848.
14. Suzdalev, I.P., Buravtsev, V.N., Maksimov, Yu.V., Zharov, A.A., Imshennik, V.K., Novichikhin, S.V., and Matveev, V.V., *J. Nanopart. Res*., 2003, vol. 5, p. 485.
15. Suzdalev, I.P., Maksimov, Yu.V., Imshennik, V.K, Novichikhin, S.V., Matveev, V.V., Gudilin, E.A., Chekanova, A.P., Petrova, O.S., and Tret'yakov, Yu.D., *Ross. Nanotehnol*., 2007, vol. 2, nos. 5–6, p. 73.
16. Dzyaloshinskii, I.E., Zh. Eksp. Teor. Fiz., 1957, vol. 33, p. 1454.
17. Schulze, G., *Metallophysics*, Berlin: Academic, 1967.
18. Hirth, J.P. and Lothe, J., *Theory of Dislocations*, New York: McGraw-Hill, 1968.
19. Valiev, R.Z., Korznikov, A.V., and Mulyukov, R.R., *Fiz. Magn. Mater*., 1992, vol. 73, p. 70
20. Taylor, K.N.R. and Darby, M.I., *Physics of Rare Earth Solids*, London: Chapman and Hall, 1972.